

ORIGINAL ARTICLE

Astrocytic water channel aquaporin-4 modulates brain plasticity in both mice and humans: a potential gliogenetic mechanism underlying language-associated learning

J Woo^{1,2,14}, JE Kim^{3,4,14}, JJ Im^{4,5,14}, J Lee^{1,15}, HS Jeong⁶, S Park¹, S-Y Jung^{1,2}, H An^{1,7,8}, S Yoon⁴, SM Lim⁹, S Lee^{4,5}, J Ma^{4,5}, EY Shin^{3,4}, Y-E Han^{1,2}, B Kim^{4,5}, EH Lee¹⁰, L Feng¹, H Chun¹, B-E Yoon^{1,11}, I Kang^{3,4}, SR Dager^{7,8}, IK Lyoo^{3,4,12} and CJ Lee^{1,2,13}

The role of astrocytes in brain plasticity has not been extensively studied compared with that of neurons. Here we adopted integrative translational and reverse-translational approaches to explore the role of an astrocyte-specific major water channel in the brain, aquaporin-4 (AQP4), in brain plasticity and learning. We initially identified the most prevalent genetic variant of *AQP4* (single nucleotide polymorphism of rs162008 with C or T variation, which has a minor allele frequency of 0.21) from a human database ($n = 60\,706$) and examined its functionality in modulating the expression level of *AQP4* in an *in vitro* luciferase reporter assay. In the following experiments, *AQP4* knock-down in mice not only impaired hippocampal volumetric plasticity after exposure to enriched environment but also caused loss of long-term potentiation after theta-burst stimulation. In humans, there was a cross-sectional association of rs162008 with gray matter (GM) volume variation in cortices, including the vicinity of the Perisylvian heteromodal language area (Sample 1, $n = 650$). GM volume variation in these brain regions was positively associated with the semantic verbal fluency. In a prospective follow-up study (Sample 2, $n = 45$), the effects of an intensive 5-week foreign language (English) learning experience on regional GM volume increase were modulated by this *AQP4* variant, which was also associated with verbal learning capacity change. We then delineated in mice mechanisms that included AQP4-dependent transient astrocytic volume changes and astrocytic structural elaboration. We believe our study provides the first integrative evidence for a gliogenetic basis that involves AQP4, underlying language-associated brain plasticity.

Molecular Psychiatry advance online publication, 27 June 2017; doi:10.1038/mp.2017.113

INTRODUCTION

Brain volume increases in parallel to brain plasticity in response to environmental demands.^{1,2} Human neuroimaging studies can detect regional increases in brain volume induced by experience or learning: for example, after juggling training,³ video gaming⁴ or intensive training to be qualified as a London taxi driver.^{5,6} These plasticity-related changes in brain volume have also been documented in the rodent brain after prolonged exposure to an enriched environment (EE)^{7,8} and in the avian brain during food-storing season.^{9,10} There have been numerous reports suggesting that neuropil increase, neuronal synaptogenesis and neurogenesis underlie these experience-driven brain volumetric changes.⁷ The involvement of glial cells in brain plasticity and associated learning has some evidence in support, including the well-established role of oligodendrocytes in activity-dependent myelination.¹¹ Although controversial, there are also reports of an increased

glia-to-neuron ratio in the parietal lobe of Albert Einstein's brain.^{12,13} Evidence for an increased astrocyte-to-neuron ratio in higher vertebrates and its correlation with higher cognitive capacity further lends support to the idea that astrocytes may serve an important role in brain plasticity and learning, although the exact mechanism underlying this proposition has been largely untested.

Water and astrocytes are undoubtedly two major components of the brain. Yet, water movement through the astrocytic water channel has only been studied in terms of fluid homeostasis, waste clearance and associated pathological states, such as brain edema.^{14,15} In this study, we sought to investigate the critical role of water, astrocytes and the channel that connects the two entities, aquaporin-4 (AQP4), in the core physiology and function of the brain—brain plasticity, particularly with regard to higher cognitive function in both mice and humans. AQP4, a member of

¹Center for Neural Science and Functional Connectomics, Korea Institute of Science and Technology (KIST), Seoul, Republic of Korea; ²Neuroscience Program, University of Science and Technology (UST), Daejeon, Republic of Korea; ³Department of Brain and Cognitive Sciences, Scranton College, Ewha Womans University, Seoul, Republic of Korea; ⁴Ewha Brain Institute, Ewha Womans University, Seoul, Republic of Korea; ⁵Interdisciplinary Program in Neuroscience, College of Natural Sciences, Seoul National University, Seoul, Republic of Korea; ⁶Department of Radiology, Incheon St. Mary's Hospital, College of Medicine, The Catholic University of Korea, Seoul, Republic of Korea; ⁷Department of Radiology, University of Washington, Seattle, WA, USA; ⁸Department of Bioengineering, University of Washington, Seattle, WA, USA; ⁹Department of Radiology, College of Medicine, Ewha Womans University, Seoul, Republic of Korea; ¹⁰Green Cross Laboratories, Yongin, Republic of Korea; ¹¹Department of Nanobiomedical Science, Dankook University, Cheonan, Republic of Korea; ¹²Graduate School of Pharmaceutical Sciences, Ewha Womans University, Seoul, Republic of Korea and ¹³KU-KIST, Graduate School of Convergence Technology, Korea University, Seoul, Republic of Korea. Correspondence: Professor IK Lyoo, Ewha Brain Institute and Department of Brain and Cognitive Sciences, Ewha Womans University, 52 Ewhayeodaegil, Seodaemun-gu, Seoul, Republic of Korea or Dr CJ Lee, Center for Glia-Neuron Interaction, Korea Institute of Science and Technology, 39-1 Hawolgokdong, Seongbuk-gu, Seoul, Republic of Korea.
E-mail: inkylyoo@ewha.ac.kr or cjl@kist.re.kr

¹⁴These authors contributed equally to this work.

¹⁵Current address: Division of Functional Food Research, Korea Food Research Institute, Seongnam, Republic of Korea.

Received 7 September 2016; revised 21 March 2017; accepted 17 April 2017

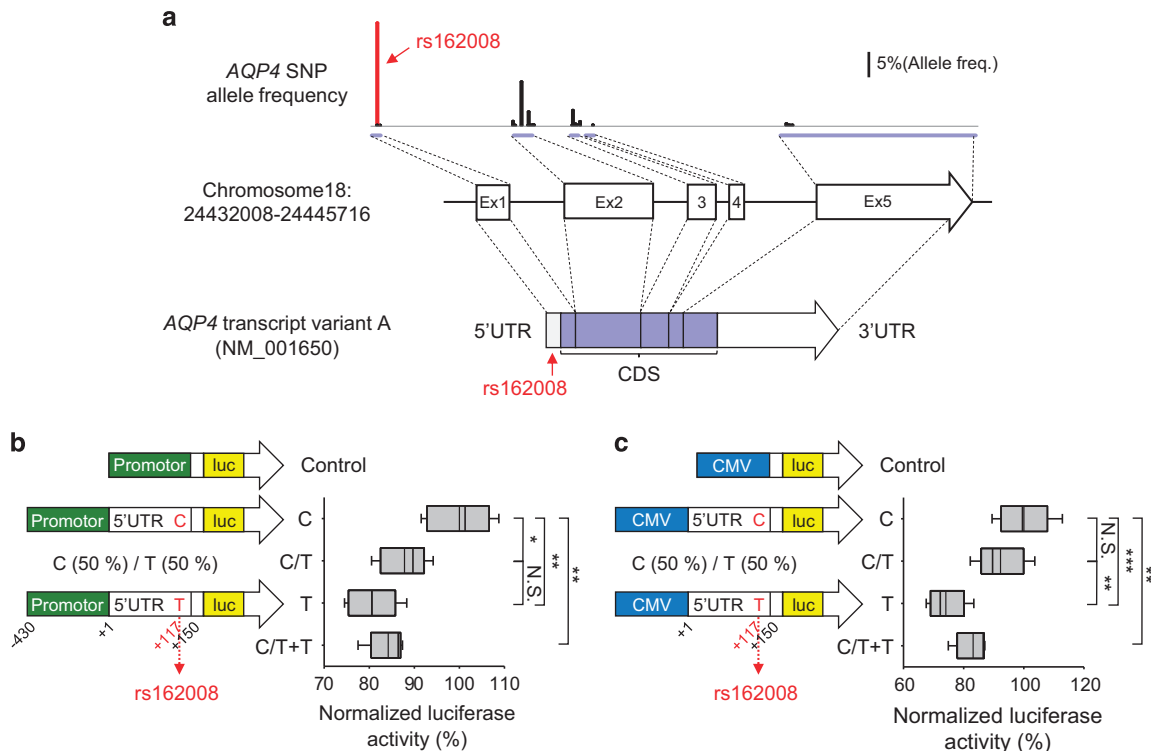


Figure 1. Rs162008 regulates *AQP4* expression. **(a)** Chromosomal information for *AQP4* (middle, bottom) and allele frequency plot of *AQP4* single-nucleotide polymorphisms (SNPs) including rs162008 (upper). **(b, c)** Results from *in vitro* luciferase assays showing that C variation at rs162008 has significantly higher expression of luciferase than the T variant. Vector information representing location of promoter and 5' untranslated region (UTR; shown on the left). Arrow indicates the location of rs162008 having different single nucleotide (C or T). The left, middle and right vertical lines of the box correspond to the 25th, 50th and 75th percentiles, respectively. The whiskers extend to show the 10th and 90th percentiles. The thin vertical line in the box represents arithmetic mean. Luciferase activity comparisons between vectors having C only (C), co-transfection of C and T (C/T), T only (T) and sum of C/T and T (C/T+T) upon *AQP4* promoter **(b)** and cytomegalovirus promoter **(c)** after subtraction of control vector and normalization to C nucleotide (* $P < 0.05$, ** $P < 0.01$, *** $P < 0.001$, one-way analysis of variance, Tukey's test, $n = 5$ for each condition). NS indicates a non-significant difference ($P > 0.05$). Error bars represent s.e.m.

13 aquaporin family, serves as a bidirectional water transporter with predominant expression in astrocytes.¹⁶ *AQP4* is also enriched in ependymocytes lining the cerebrospinal fluid-filled ventricles as well as astrocytic plasma domains adjacent to the brain microvessels or the pia.¹⁶ Moreover, it is expressed in perisynaptic astrocytic processes, insinuating its role in regulating synaptic plasticity, in addition to its well-known function in water homeostasis.^{1,2}

The *AQP4* gene is located at chromosome 18q11.2-12.1. The petit arm of chromosome 18 is the range of genetic loci where genome-wide linkage analysis studies have reported evidence of suggestive linkage with various neuropsychiatric conditions, such as schizophrenia,¹⁷ bipolar disorder,^{18,19} attention-deficit hyperactivity disorder,²⁰ developmental delay, intellectual disability²¹ and autism spectrum disorders.²² These disorders also exhibit brain plasticity dysfunction as well as cognitive deficits.²³ However, the potentially phylogenetically preserved roles of *AQP4* have not been systematically investigated in the pathogenesis of these disorders, let alone in brain plasticity.

To unravel the role of astrocytic *AQP4* in brain plasticity, we undertook a highly integrated translational (from bench to human) and reverse-translational (from human to bench) research approach. Most medical therapeutics currently in use were first developed and tested in animals and then validated in human clinical trials. Nevertheless, even the most highly cited animal studies (>600 citations) required a median of >14 years for potential translation.²⁴ A more integrative approach in which basic and clinical research communicates at an earlier stage would be ideal. This would expedite the application of newfound basic

findings to humans and the provision of insight from human findings for target refinement, enhancing human relevance of basic research.

We focused on the *AQP4* gene, which is specifically expressed in astrocytes as the major water channel of the brain.^{1,2} We performed a series of *in vitro*, *in vivo* animal and *in vivo* proof-of-concept human neuroimaging and neuropsychological studies in two independent samples (Supplementary Figure S1). The main objective of this study is to elucidate the role of *AQP4* in brain plasticity and associated cognitive function both in mice and humans.

MATERIALS AND METHODS

Overall study design

The current study is composed of nine sets of experiments and analyses (Supplementary Figure S1). The first step was the identification of *AQP4* common single-nucleotide polymorphism (SNP) using the Exome Aggregation Consortium database, the largest collection of human DNA sequencing data from >60 000 people.²⁵ Second, in an *in vitro* luciferase reporter assay, we tested whether this genetic variation causes *AQP4* expression-level changes. Third, we examined the effects of *AQP4* knockdown on hippocampal volumetric changes after exposure to EE in mice, as well as on long-term potentiation (LTP) after theta-burst stimulation (TBS) in hippocampal slices. Afterwards, we analyzed the differences in gray matter (GM) volume between individuals with different *AQP4* SNP genotypes using cross-sectional human genetic neuroimaging data (Sample 1, $n = 650$). Then another prospective follow-up study in humans (Sample 2, $n = 45$) with an intensive foreign word learning interventional design was conducted to assess the effects of genetic

variation on brain plasticity. Finally, the potential underlying mechanisms were identified in detail back at the bench using *in vitro* and *in vivo* animal studies. We undertook the aforementioned experiments in a methodical manner, in which specific hypotheses for each step were derived from the results of the preceding studies (Supplementary Figure S1).

In silico and *in vitro* assessments

SNP selection. First, *in silico*, we identified the most prevalent SNP using the Exome Aggregation Consortium database.²⁵ Among the available reference SNPs, only rs162008 had an allele frequency >0.20 (Figure 1a). Choosing this SNP allowed an adequate sample size for each genotype group in conducting proof-of-concept human experiments. For the detailed method of the luciferase reporter assay, please see Supplementary Information.

Effect of AQP4 genetic variation on brain volumetric plasticity in mice

Animals and housing. Adult (8–10 weeks) C57BL/6 (B6) and glial fibrillary acidic protein-green fluorescent protein (GFAP-GFP; Balb/C strain) mice of each sex and genotype were used. All experimental procedures were performed in accordance with the institutional guidelines of the Korea Institute of Science and Technology (KIST), Seoul, Republic of Korea (approval number: 2016-051).

AQP4 short hairpin RNA (shRNA) vector construction and reverse transcription-PCR. shRNA for mouse AQP4 (NM_009700) was targeted at nucleotides 317 to 337 (5'-gcacacgaaagatcagcatcg-3') and inserted into the pSicoR system.²⁶ Gene silencing of AQP4 was tested by reverse transcription-PCR. For gene silencing of AQP4, lentivirus carrying AQP4 shRNA was infected into primary cultured astrocytes 4 days after culture. Approximately 5 days after infection, the total RNA was prepared using TRIzol reagent (Invitrogen, Carlsbad, CA, USA). cDNA was synthesized using SuperScript III Reverse Transcriptase (RT, Invitrogen).

Virus injection

Mice (8–10 weeks old) were anesthetized by intraperitoneal injection of 2% avertin (20 $\mu\text{l g}^{-1}$) and placed into stereotaxic frames. pSicoR lentivirus (4.6×10^{11} LPS ml^{-1} titer, LPS: lenti particles) containing AQP4 shRNA was loaded into a microdispenser (VWR, Radnor, PA, USA) and injected bilaterally into the hippocampal CA1 region (–1.7 mm AP, ± 1.7 mm ML, 1.8 mm DV from the dura) at a rate of 0.3 $\mu\text{l min}^{-1}$ (total 2 μl) with a 25 μl syringe using a syringe pump (KD Scientific, Holliston, MA, USA). The stereotaxic coordinates of the injection site were 1.7 mm away from the bregma and the depth was 1.9 mm beneath the skull.

Enriched environment. B6 mice (8–10 weeks old) were housed from weaning in an EE and standard conditions (STD) for 1 month. The EE was equipped with various toys, including tunnels, a wood ladder, igloo and running wheel. Toys were made of different forms of plastic, wood and metal, were of different colors and were changed periodically.²⁷

Measurement of hippocampal volume. Mice were transcardially perfused with 10% formalin and then brains were extracted and further fixed in 10% formalin at room temperature. Right or left hemispheres were chosen at random beforehand. Coronal sections (40 μm thickness) were cut through the entire hippocampus region using a vibratome (Leica VT1200S, Wetzlar, Germany). Brain slices were mounted onto slides and stained with cresyl violet according to the general Nissl staining procedure. Stained slices were photographed and then converted into eight-bit images. The boundaries of the CA1 and dentate gyrus (DG) were delineated in the following way: Two lines were drawn to establish a perimeter that excluded the DG. One line was passed through the lateral most ends of the DG and extended until it reached the CA1. The other line was extended from the medial most tip of the DG to the corner where the CA1 and the dorsal third ventricle meet. This perimeter, consisting of the boundary of the CA1, DG and the two lines drawn, essentially surrounds a subregion of the Ammon's horn. The area of the resulting perimeter was measured with the ImageJ software (US National Institutes of Health, Bethesda, MD, USA). This area was then multiplied by the slice thickness to give an estimate of the volume. The measurement was based on the classic mathematical principle of Cavalieri²⁸ with our modification as described above.

Slice preparation, electrophysiology, whole-cell synaptic recordings of LTP and other methods. Hippocampal slices were prepared from P56 to P70 mice and LTP in CA1 pyramidal neurons was measured as previously described.^{29,30} Detailed methods of passive avoidance test and immunohistochemistry are included in Supplementary Information.

Sample 1: correlative effect of AQP4 rs162008 on human brain volumetric plasticity

Participants. Both study protocols for human neuroimaging studies were approved by the Institutional Review Board of Ewha Womans University (approval numbers: 67-7 and 102-14). Healthy volunteers ($n=650$, Supplementary Table S1) were enrolled through local advertisements. Subjects provided written informed consent after detailed explanation of the study protocol that included neuroimaging, behavioral assessment and genetic testing. The inclusion criteria were ages 18–65 years, absence of psychotropic medication and normal intelligence quotient, as evaluated using the Korean version of the Wechsler Abbreviated Scale of Intelligence.³¹ Exclusion criteria were: (1) current axis I psychiatric diagnosis according to the Structured Clinical Interview for the Diagnostic and Statistical Manual of Mental Disorders-IV, (2) current or past severe medical or neurological illnesses, (3) contraindications for magnetic resonance (MR) imaging. The sample size was determined using the expected group ratio of 1.66:1 and the effect size reported in Huang *et al.*,³² with an α level of 0.05 and a β level of 0.9.

DNA extraction and SNP genotyping. Human blood samples were collected in EDTA tubes, and genomic DNA was extracted with a Blood Genomic DNA Extraction Kit (Invitrogen) according to the manufacturer's instructions. The concentration and purity of all DNA samples were determined. Genotyping of the AQP4 SNP was performed using the TaqMan SNP genotyping probe (Applied Biosystems, Waltham, MA, USA). PCR signals and fluorescence signals were detected and analyzed with ABI StepOne 01 (Applied Biosystems). Genotyping was performed after all clinical, neuroimaging and neuropsychological assessments were completed, so that the genotype group membership of each participant could be double-blinded. Exact test was performed to calculate Hardy–Weinberg equilibrium P -values considering the modest sample size of Sample 2.

Neuroimaging data acquisition and analyses. All MR scans were performed using a 3.0 Tesla Achieva MR scanner (Philips Medical Systems, Best, The Netherlands) equipped with a 32-channel head coil, located at the Ewha Brain Institute. For the acquisition parameters, please see Supplementary Information.

T1-weighted images were analyzed using an optimized voxel-based morphometry protocol using FSL version 5.0.2.1.^{33,34} First, using a brain extraction tool, non-brain tissues were removed, with T2-weighted images available to optimize the skull-stripping process.³⁵ Tissue segmentation was performed and the resulting GM segmented images were registered to the Montreal Neurologic Institute 152 standard spaces using non-linear registration. A symmetrical, study-specific GM template was created by averaging and flipping these resulting images. All native GM images were then non-linearly normalized to the study-specific template and smoothed using Gaussian kernels with a sigma of 3 mm. A mask including only voxels for which the group-averaged values were >0.15, but excluding the cerebellum and the brain stem, was applied.

Statistical analyses

For MR imaging data analyses, a general linear model was used.³⁶ The variable of interest was the genotype group (CC or CT/TT genotype groups), while age and sex were covariates. Multiple comparisons were corrected using the 3dClustSim implemented in AFNI,³⁷ which generates a random field of noise with Monte Carlo simulations to determine significant clusters at $P < 0.05$. Residual images were used to derive smoothness parameter.^{38,39} The average density values of the clusters with significant differences were extracted for testing associations with scores from the Controlled Oral Word Association Test (COWAT).⁴⁰ Regression analysis was used to test associations between the average density value and the COWAT score. Statistical analyses were conducted using Stata (version 13.1: Stata, College Station, TX, USA). The statistical methods for sensitivity analyses are described in Supplementary Information.

Sample 2: effect of AQP4 genetic variation on experiential brain GM volume changes in humans

Participants and protocol. Subjects ($n=85$) were screened and provided written informed consent prior to study participation. The subjects were selected for a 'Learner' group ($n=60$) and a control group ($n=25$), based upon whether or not the participant planned to take the Graduate Record Exam (GRE) for the purpose of entering graduate school in the United States. The inclusion criteria were: (1) ages 20–40 years and (2) no prior experience of studying for the GRE. Exclusion criteria were: (1) any current axis I psychiatric diagnosis according to the Structured Clinical Interview for the Diagnostic and Statistical Manual of Mental Disorders-IV, (2) personality disorder diagnosis based on the Personality Diagnostic Questionnaire-4, (3) current pregnancy, (4) current or past severe medical illnesses, (5) intelligence quotient < 90 , or (6) contraindications for MR imaging. All participants were native Korean speakers. The control group was age and sex matched. In the Learner group, 15 enrolled subjects were excluded due to exclusion criteria ($n=3$), time conflicts ($n=3$) or incidental radiological findings ($n=4$). Five participants were dropped due to non-compliance to the protocol ($n=1$) and time conflicts ($n=4$). Forty-five participants completed the intensive learning procedures and data from these participants were included in the analyses. For the control group, one participant who had an incidental radiological finding and one who refused to participate in the follow-up visit were excluded in the final analyses.

The intensive learning protocol consisted of a 1-h lecture on the etymology of words from the GRE verbal reasoning section followed by 4-h self-study sessions, 6 days per week. For each self-study session, a list of 120 words were given for memorizing. The number of words were selected based on a prior report that participants showed increased cortical thickness and hippocampal volumes after learning > 3000 foreign words.⁴¹ At the end of each day, participants were presented with a written survey in which they recorded the time they had actually spent studying.

The California Verbal Learning Test^{42,43} was administered to all participants at baseline and at end point. We calculated the inverse z-score changes in total intrusion errors, a sensitive measure of performance level in word learning with the least practice or ceiling effects⁴⁴ after adjusting for baseline values. Regression analysis was used to test the association between the average density value and the z-score change in the word learning performance level.

For 44 of the participants in the Learner group, 2:1 matching was performed. For the remaining one Learner group participant, 1:1 matching was performed. This matching information was treated as a random effect. Characteristics of these participants are shown in Supplementary Table S2.

Neuroimaging data acquisition and analyses. For MR imaging data acquisition, the identical imaging parameters and hardware were used as for the cross-sectional study ($n=650$). Following the brain extraction step described previously, all brain-extracted neuroimages were visually inspected and any remaining non-brain tissues were removed manually by an experienced imaging researcher who was blind to group assignment, demographic or genotypic information of the participants. The same normalization, smoothing and masking steps were applied, as detailed previously, prior to voxel value extraction.

For linear mixed-effects modeling, each voxel value was included as the dependent variable, the fixed-effect independent variable was total study time, and the random-effect variable was participant ID. Voxels having significant association with total study time were identified. Multiple comparison concerns were addressed by a more conservative application of the false discovery rate at $q < 0.05$ with a cluster extent threshold $k > 100$ voxels. The average density values of these regions were extracted for further analyses. Interaction effects between each genotype group and total study time for the extracted average GM density values were tested using linear mixed-effects modeling that controlled for the fixed effect of baseline values. Methods of sensitivity analyses are included in Supplementary Information.

Mechanisms underlying the AQP4-modulated brain volumetric plasticity

Intrinsic optical signal (IOS) imaging. Submerged slices were transilluminated using a controlled infrared (IR) light source with optical filter (775 nm wavelength, Omega Filters (Brattleboro, VT, USA)), and images from the stratum radiatum of hippocampal CA1 region were taken using a microscope (Olympus, BX50W; Tokyo, Japan) equipped with a digital CCD camera (Hamamatsu, ORCA-R2; Hamamatsu, Japan). A series of 80

images s^{-1} were acquired following 1 s of 20 Hz electrical stimulation. The relative change of transmittance ($\Delta T/T$) was normalized to baseline (average of five images). Decay of the IOS was measured by averaging the last 10 s of the response after dividing responses with peak response. Imaging Workbench software (INDEC BioSystems, Santa Clara, CA, USA) was used for image acquisition and analyses.

Single-cell volume measurement. Astrocyte images from brain slices of GFAP-GFP mice were taken using a confocal microscope (Zeiss, LSM 780; Oberkochen, Germany) and acquired with z-stacking (5 stacks per 5–6 μm). Series of 60 images per 5 s were acquired after 1 s of 20 Hz electrical stimulation. Measurement of the resulting perimeter area was performed using the ImageJ software (US National Institutes of Health). The relative change was normalized to baseline (average of five images). For AQP4 gene-silencing experiments, we injected adenoviral (mCherry-tagged) control and AQP4 shRNA into the CA1 stratum radiatum region in GFAP-GFP mice. Neurons were identified by the presence of mCherry fluorescence and their characteristic morphology was confirmed from control shRNA-infected brain slices.

RESULTS

We tested *in vitro* whether this SNP, which is located in 5'UTR (untranslated region), is functional at the transcription level. We performed a luciferase assay with vectors containing the AQP4 promoter (Figure 1b) or the cytomegalovirus promoter (Figure 1c) and 5'UTR with C/T variation at rs162008. We found that rs162008 with T variation resulted in reduced luciferase expression compared with C variation, supporting that rs162008 is a functional regulatory genetic polymorphism.

Next we examined whether there was a potential effect of AQP4 on brain plasticity through an experimental perturbation of AQP4 in mice exposed to EE. To modulate the functional expression of AQP4, we developed a lentivirus carrying a shRNA specific for AQP4 (Supplementary Figure S2), injected it bilaterally into CA1 hippocampus of mice for acute gene-silencing and then exposed the mice to EE for 30 days (Figures 2a and b). In contrast to the control shRNA-injected mice, EE-induced increases in hippocampal size were not observed in AQP4 shRNA-injected mice (Figures 2b and c).

It has been previously reported that AQP4 knockout mice show impaired neurotrophin-dependent synaptic plasticity and selective spatial memory impairment.⁴⁵ To examine this with our gene-silencing approach, we measured the TBS-induced LTP and spatial memory from AQP4 shRNA-injected mice. We observed complete loss of LTP (Figures 2d and e) and impaired context-dependent memory (Figures 2f and g) in AQP4 shRNA-injected mice compared with control shRNA-injected mice.

To assess functionality of AQP4 in *in vivo* humans, we first utilized a neuroimaging-genetics data set of healthy individuals ($n=650$) to compare high-resolution brain MR imaging data of individuals with the CC genotype ($n=236$) with those having the CT or TT genotype ($n=414$) at the rs162008 locus. Characteristics of participants are presented in Supplementary Table S1. There were no differences between the CC genotype and the CT or TT genotype groups, in age ($t = -0.41$, $P = 0.68$), sex (Fisher's exact $P = 0.93$), handedness (Fisher's exact $P = 0.42$), intelligence quotient as measured with Wechsler Abbreviated Scale of Intelligence ($t = 1.24$, $P = 0.21$), years of education ($t = 0.41$, $P = 0.68$), semantic ($t = 0.91$, $P = 0.36$) and phonemic ($t = 1.41$, $P = 0.16$) verbal fluency level and the intracranial volume ($t = 0.68$, $P = 0.50$), as assessed by Student's *t*-test and Pearson's chi square test for continuous and categorical variables, respectively. All participants were psychotropic medication-free. We found that individuals with the CC genotype had greater GM volumes in brain regions encompassing the bilateral central opercular cortex, precuneus and adjacent areas and that there were no regional reductions in GM volume relative to the CT or TT genotype group (Figures 3a, b and Supplementary Table S3). Regions observed to have increased GM

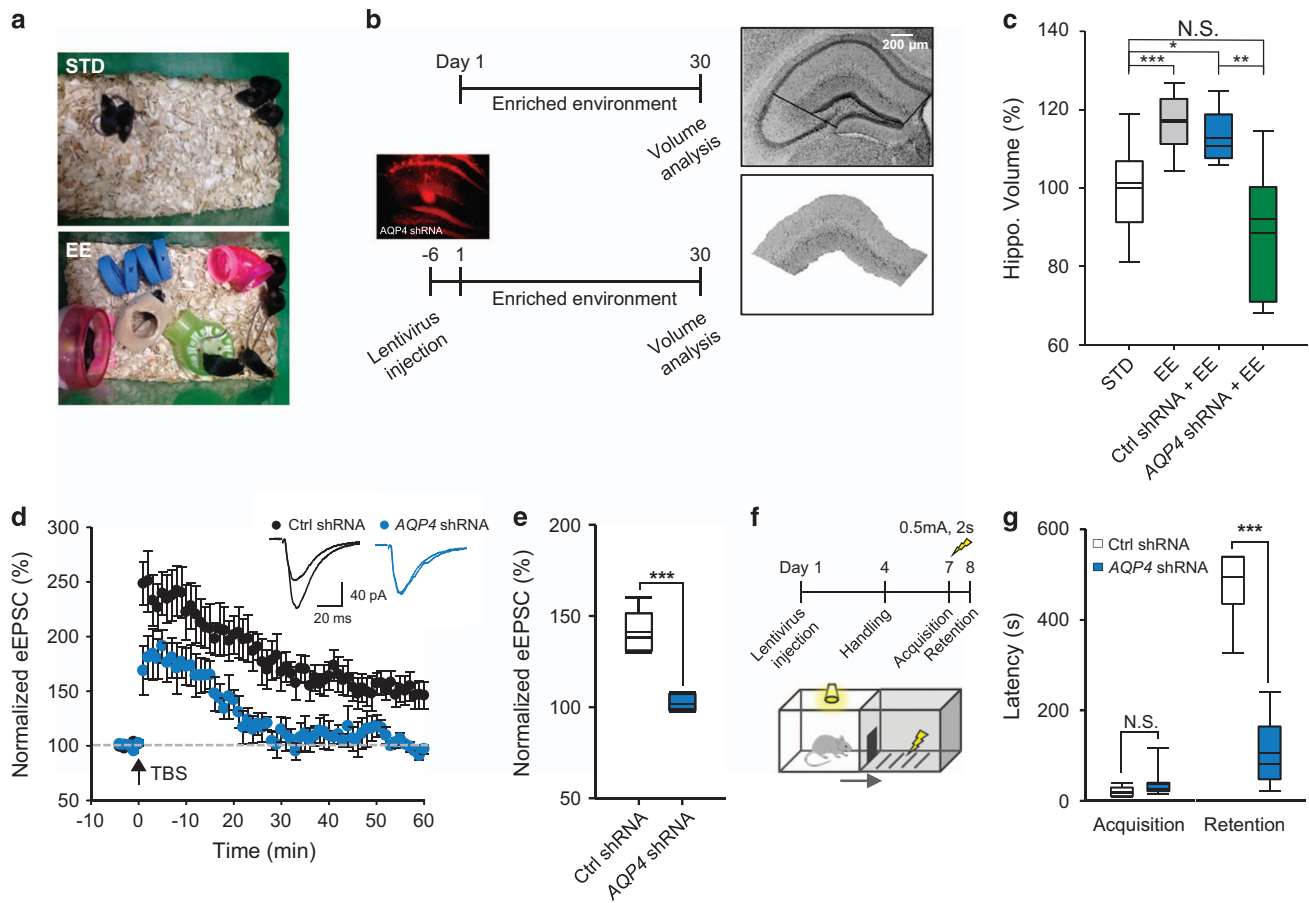


Figure 2. Effects of *AQP4* on brain plasticity in mice. **(a)** Cages for standard condition (STD) and enriched environment (EE). **(b)** Experimental design for EE and volume measurement (left) and representative image for hippocampal volume measurement (right). Inset: representative image for *AQP4* shRNA-infected brain slice. **(c)** Comparisons of the hippocampal volume in each condition ($*P < 0.05$, $**P < 0.01$, $***P < 0.001$, one-way analysis of variance, Tukey's test; $n = 9$ (STD), 10 (EE), 8 (Ctrl shRNA), 10 (*AQP4* shRNA)). NS indicates a non-significant difference ($P > 0.05$). Error bars represent s.e.m. **(d)** Theta-burst stimulation induced long-term potentiation (LTP) from mice expressing control shRNA and *AQP4* shRNA. **(e)** Summary bar graph of LTP (averaging responses for the last 10 min, $***P < 0.001$, Student's *t*-test; $n = 5$ (*AQP4* shRNA), 7 (Ctrl shRNA)). **(f)** Schematic and experimental schedule for passive avoidance test. **(g)** Latency of acquisition and retention in passive avoidance test. ($***P < 0.001$, Student's *t*-test; $n = 8$ (*AQP4* shRNA), 8 (Ctrl shRNA)). **(c, e, g)** The bottom, middle and top horizontal lines of the box correspond to the 25th, 50th and 75th percentiles, respectively. The whiskers extend to show the 10th and 90th percentiles. The thin horizontal line in the box represents arithmetic mean. eEPSC, evoked excitatory postsynaptic current.

volume included the language-associated heteromodal cortices, where experience-dependent brain volumetric plasticity is particularly evident. Increased volumes in these regions were associated with greater semantic verbal fluency, measured using the COWAT (Figure 3c). Assessing sample-specific factors that might influence these results, there was no evidence for confounding effects (Supplementary Figure S3).

There has been a plethora of evidence that the Perisylvian cortex, where GM volume showed an association with the *AQP4* genetic variation in the cross-sectional sample ($n = 650$) of the current study, is a core structure involved in language representation.^{46,47} In addition, we tested the association between GM variability in this region and semantic verbal fluency test scores and found a linear relationship (Figure 3c). Thus we extended our investigation of this genotypic functional association through a prospective study that evaluated healthy young adults (Supplementary Table S2) enrolled in an intensive foreign language (English) course over 5 weeks (5.1 ± 0.1 weeks, $n = 45$; Figure 3d). This intervention has high ecological validity as it reflects our learning experiences in real-world settings.

High-resolution structural brain MR imaging data were obtained before and at completion of the intensive language course

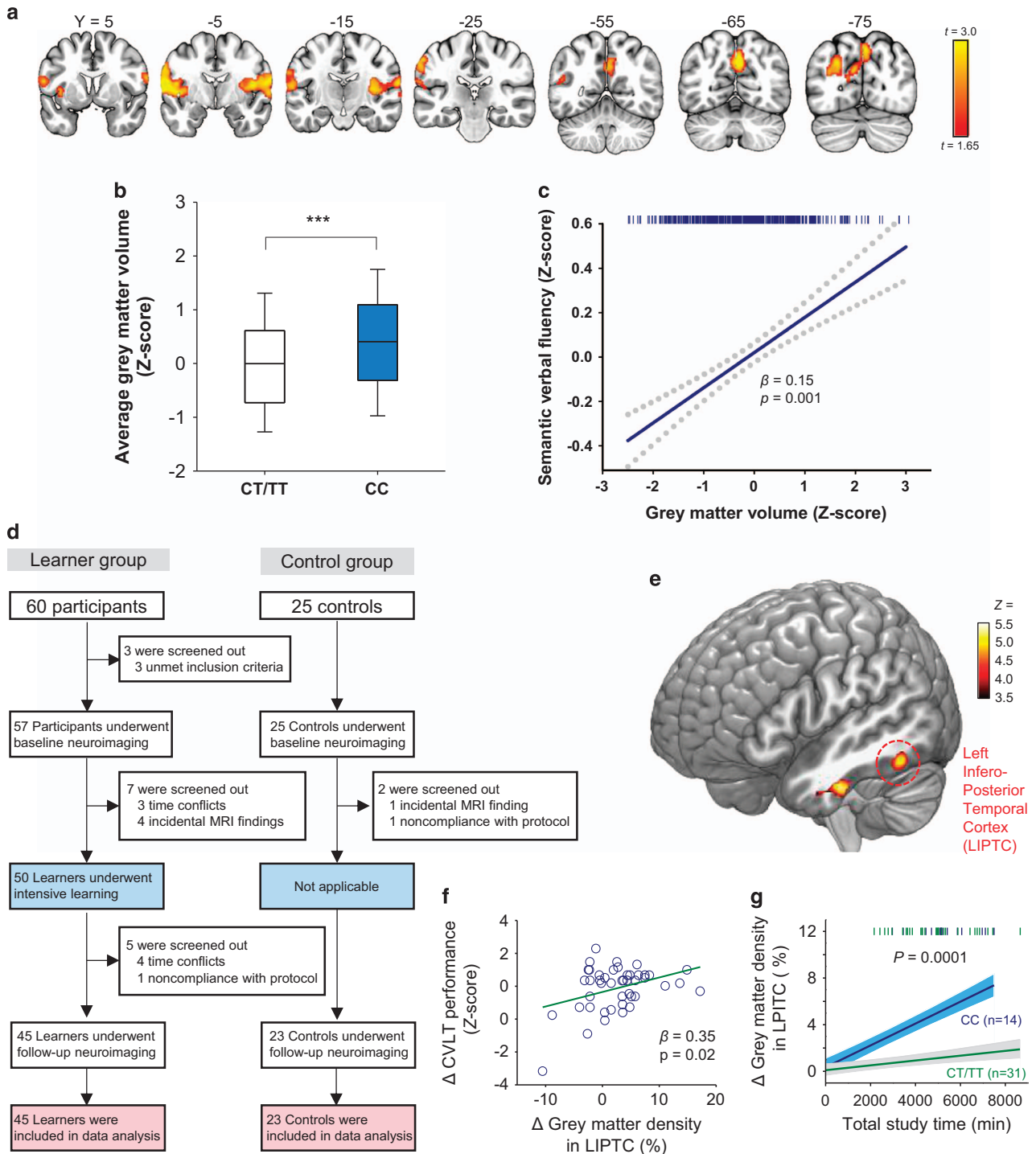
(Figure 3d). We first examined whether there were regional increases in cerebral GM volume following intensive language learning that were positively correlated with the amount of total study time. At a $P < 0.05$ after false discovery rate correction,⁴⁸ we found two regions of increased cerebral GM volume that encompassed the left infero-posterior temporal cortex (LIPTC) and left fusiform cortex (Figure 3e and Supplementary Table S4). The robustness of this association was tested using sensitivity analyses (Supplementary Figure S4). The magnitude of increased GM volume in the LIPTC (Figure 3e) was positively associated with the extent of performance improvement on the California Verbal Learning Test (Figure 3f).

We next investigated the relationship between rs162008 genotype and GM volume increases in the LIPTC. The CC group showed a greater increase in LIPTC GM volume, compared with the CT or TT group (Figure 3g). These results suggest that *AQP4* rs162008 is associated with experiential GM increases from language-associated learning. Hardy–Weinberg equilibrium *P*-values of this SNP were 0.36 and 0.54 for Samples 1 and 2, respectively.

Findings of the association between *AQP4* genetic variation and volumetric plasticity of the human brain in both cross-sectional

and prospective human studies led to further animal model investigation of underlying mechanisms. We first detected and visualized the neuronal activity (20 Hz, 1 s) induced transient volume changes in acutely prepared hippocampal slices using IOS imaging with an IR wavelength (775 nm) light source (Supplementary Figure S6a).⁴⁹ Using a variety of synaptic transmission inhibitors, we confirmed that IOS-detected transient volume changes were primarily mediated by excitatory synaptic transmission, as previously suggested (Supplementary Figures S6b–g).²⁹ To determine the cellular source of IOS and the role of

AQP4 in transient volume changes, we measured IOS in brain slices and single-cell volumes using confocal microscopy before and after gene silencing of *AQP4* (Figures 4a and d). We found almost complete abolishment of IOS (Figures 4b and c) and reduction of single astrocytic cell volume (Figures 4e and f) by *AQP4* shRNA compared with control shRNA. In contrast, the volume change in neurons was negligible, similar to that of unstimulated astrocytes or that of *AQP4* shRNA-expressing astrocytes following stimulation (Figure 4f and Supplementary Figure S7).



To test whether the *AQP4*-dependent brain plasticity observed in EE mice (Figures 2a–c) is accompanied by astrocytic structural changes, we employed immunohistochemistry techniques to examine the role of *AQP4* in structural plasticity of mice under standard housing conditions. As expected, *AQP4* shRNA-expressing astrocytes showed significantly reduced branching as measured by Sholl analysis, compared with control shRNA-expressing astrocytes (Figures 4g–i). Morphological changes were similarly measured in EE mice with demonstration of enhanced GFAP intensity and increased astrocytic branching in control EE mice compared with non-EE mice, whereas the EE mice with *AQP4* shRNA expressing astrocytes showed markedly reduced effects (Figures 4j–m). These *AQP4*-dependent morphological changes in EE-exposed mice were also accompanied by increase in dynamic range of transient volume change (Figures 4n, o and Supplementary Figure S8) that, in part, may reflect augmentation of the interface between neurons and astrocytes. *AQP4* gene silencing, on the other hand, did not affect the level of cell viability (Supplementary Figure S9).

DISCUSSION

Here a unified approach integrating *in vitro*, *in vivo/ex vivo* animal and *in vivo* proof-of-concept human studies²⁴ is presented that implicates the involvement of astrocytic *AQP4* in brain plasticity and learning. Taken together, these results suggest that experience-dependent increases in GM volume, observed both in mice after EE exposure and in humans following intensive language learning, involve structural changes in astrocytes via *AQP4*. These findings provide a complex model for understanding the involvement of astrocytes,⁵⁰ as well as neurons,⁷ in language-associated brain plasticity and learning.

In prior studies, *AQP4* has been linked to synaptic plasticity and memory through knockout mouse models.^{45,51–53} *AQP4* null knockout mice showed impaired TBS-induced LTP. Our results from the acute knockdown model are in line with these results, showing impaired synaptic plasticity and context-dependent memory in *AQP4* shRNA-injected mice compared with control shRNA-injected mice. The current study also provides novel evidence about the mechanisms by which this astrocytic water channel is linked to brain plasticity and learning: stimulation elicits transient volume changes of astrocytes through *AQP4*, which were found to be essential for LTP, learning and associated astrocytic branching. Moreover, the phylogenetically preserved role of this

astrocytic water channel has been demonstrated through closely linked human neuroimaging-genetics studies.

AQP1, *AQP4*, *AQP9* and *AQP11* are reported to be expressed in the brain.⁵⁴ However, as *AQP1* and *AQP9* show restricted expression and *AQP11* lacks apparent transport function,⁵⁵ *AQP4* is the major water channel in the brain. Previous studies indicate that *AQP1* is localized exclusively in the choroid plexus epithelium, while *AQP4* is expressed on the distal processes of astrocytes as well as the vascular feet, throughout the human brain under physiological conditions.⁵⁶ According to the human postmortem brain microarray data from the Allen Brain Atlas resources,⁵⁷ fronto-limbic and temporal cortical regions are where *AQP4* is most highly expressed, showing approximately 8.0 average \log_2 TPM (transcripts per million) and >6.0 \log_2 TPM for probes A_23_P107565 and A_24_P202522, respectively. However, it should be noted that *AQP4* may be one of the genes that show rapid expression changes postmortem, as a sudden loss of *AQP4* has been reported after cerebral ischemia.⁵⁸

Language- and speech-associated brain regions, where we found a positive relationship with *AQP4* genetic variation in a cross-sectional study, would be one of the most frequently activated brain areas, as our daily mental activities and higher cognitive processes would usually require language-associated functions. As shown in our findings from the electrophysiological study, *AQP4* was particularly important in experience-dependent brain plasticity such as TBS-induced LTP, rather than changing baseline cell membrane properties or basal synaptic transmission. Based on these findings along with the fact that learning advanced second language vocabulary would be an adequate and powerful environmental input that may induce anatomical brain alterations,⁵⁹ we chose to proceed with the intensive second language vocabulary learning protocol.

In this prospective study, participants reported to have studied for an average of 83.4 h. In a previous study of which participants were scanned during an English immersion program that is comprised of 56 h of training lessons (3.5 h per day, 4 day per week, for 3.5 week), the *COMT* genotype was found to moderate the association between immersion and white matter brain structure.⁶⁰ It can be inferred that the duration and intensity of our second language learning protocol along with the longitudinal follow-up study design was adequately powered. Indeed, we found significant GM increase in the LIPTC and the fusiform cortex. The critical role of the LIPTC in spelling difficult words⁶¹ and in identifying graphemes within words⁶² supports biological

Figure 3. Effects of *AQP4* rs162008 on human brain volumetric plasticity. **(a)** Results from *in vivo* human cross-sectional neuroimaging-genetics data ($n = 650$) showing that *AQP4* rs162008 CC homozygotes have greater volumes in bilateral regions including the central operculum and in the region encompassing the precuneus and the occipital cortex, than T carriers. There were no regions where CC homozygotes had smaller volumes than T carriers. Multiple comparisons were corrected using Monte Carlo simulation (please see Materials and methods section for more details). The numbers above brain slices indicate the y coordinates for coronal slices in the Montreal Neurological Institute (MNI) space. **(b)** Gray matter (GM) volume differences in these regions were depicted as modified box-and-whisker plots after z-scorization (middle). Boxes denote quartiles and whiskers indicate the 10th and 90th percentiles. Lines for arithmetic mean and 50th percentile overlap and are not discernable. GM volumes in these regions were associated with greater semantic verbal fluency ($\beta = 0.15$, $P = 0.001$). Regression (solid line) and s.e.m. lines (dotted lines) are shown. Tick marks above the graph denote data points. **(d)** Flow chart of participants included in the *in vivo* human study with a prospective design. Incidental magnetic resonance imaging findings included cavernous angioma ($n = 1$), prominently dilated perivascular space ($n = 2$), marked age-inappropriate temporal cortical thinning ($n = 1$) and old infarct in the parietal region ($n = 1$). **(e)** Brain regions of increased GM volume following intensive learning (false discovery rate-corrected $P < 0.05$, cluster extent threshold $k > 100$), superimposed on an ICBM 152 nonlinear brain template. For details of main and sensitivity analysis results, please see Supplementary Figure S4 and Supplementary Table S4. **(f)** Relationship between GM volume change of the cluster in the left infero-posterior temporal cortex (LIPTC), circled region in panel **(e)** and verbal learning performance-level change. Inverse z-score of total intrusion errors in the California Verbal Learning Test (CVLT) was used to measure verbal learning performance level. **(g)** A genetic variation (rs162008) in *AQP4* predicts changes in GM volume following intensive learning in humans. Trajectories of percentage of changes in the LIPTC GM volume following intensive learning were different between rs162008 genotype groups. The P -value for interaction effect between total study time and genotype groups, which were derived from the linear mixed-effects regression model adjusting for baseline values, is presented above the plot. Solid lines represent the linear fit of the data, whereas colored regions represent the s.e.m. Tick marks above the regression lines denote total study time in minutes for each individual. The blue color is for the CC genotype group, while the green color is for the CT or TT genotype group at rs162008. MRI, magnetic resonance imaging.

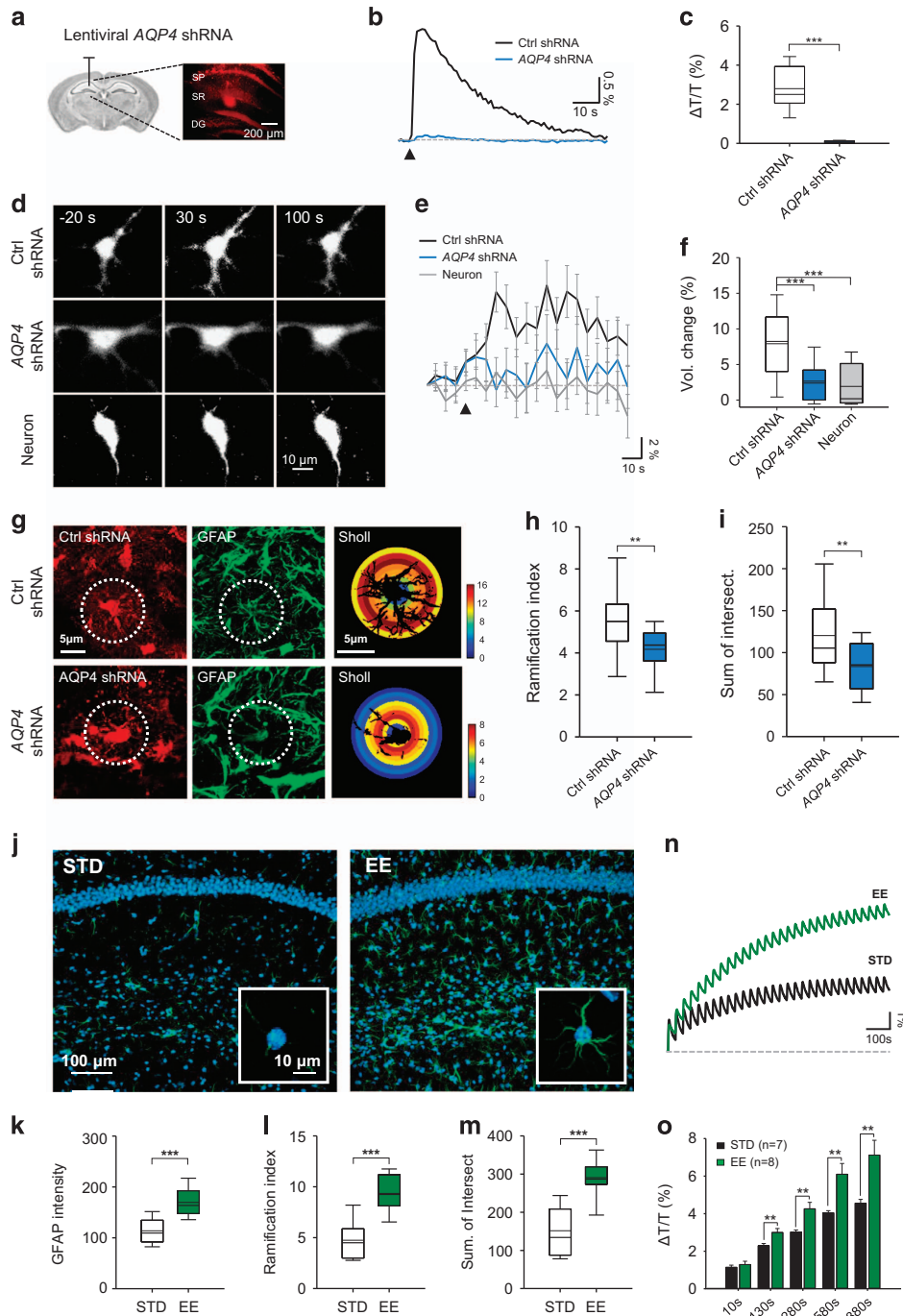


Figure 4. Mechanisms underlying the AQP4-modulated brain volumetric plasticity. **(a)** Schematic diagram showing *in vivo* injection of lentiviral AQP4 short hairpin RNA (shRNA) into the stratum radiatum of hippocampus CA1. Image on the right shows the extent of lentiviral infection by the reporter mCherry signal. **(b)** Representative trace of intrinsic optical signal (IOS) induced by neuronal activity (triangle: Shaffer collateral electrical stimulation at 20 Hz, 1 s) from CA1 hippocampal slices of mice expressing control shRNA or AQP4 shRNA. **(c)** The amplitude of IOS in these mice ($***P < 0.001$, Student's *t*-test, $n = 7$ (Ctrl shRNA); 6 (AQP4 shRNA)). **(d)** Representative images for a single astrocyte expressing control or AQP4 shRNA and a neuron. **(e)** Averaged volume changes in control or AQP4 shRNA-expressing astrocytes and neurons. **(f)** Summary bar graph of volume change. ($***P < 0.001$, one-way analysis of variance, Tukey's test, $n = 50$ (Ctrl shRNA, AQP4 shRNA); 15 (neuron)). **(g)** Immunostaining for glial fibrillary acidic protein (GFAP) in control and AQP4 shRNA expressing slices (left and middle). Dotted circle represents region of interest. Sholl analysis in astrocytes expressing control and AQP4 shRNA (right). Color scale bar indicates number of intersect. **(h, i)** Measurement of ramification index **(h)** and summation of intersect **(i)** by Sholl analysis (10 astrocytes from 2 mice per each condition, Student's *t*-test, $*P < 0.05$, $n = 10$). **(j)** Immunostaining for GFAP in sections from mice in standard condition (STD) and enriched environment (EE). Inset: magnified astrocyte; blue: 4,6-diamidino-2-phenylindole; green: GFAP. **(k–m)** Measurement of the GFAP intensity **(k)**, ramification index **(l)** and summation of intersect **(m)** by Sholl analysis from STD- and EE-exposed mice (5 slices, 10 astrocytes from 2 mice per each condition, Student's *t*-test; $**P < 0.01$, $***P < 0.001$). **(n)** Dynamic range of transient IOS in mice from STD and EE. **(o)** Measurement of IOS amplitude in each condition versus time ($**P < 0.01$, Student's *t*-test). The bottom, middle and top horizontal lines of the box correspond to the 25th, 50th and 75th percentiles, respectively. The whiskers extend to show the 10th and 90th percentiles. The thin horizontal line in the box represents arithmetic mean.

plausibility of this finding, as all participants had intensive instruction on the etymology of unfamiliar foreign words. Individuals with the CC genotype, the genotype we expected greater *AQP4* expression levels upon cellular activity through the luciferase reporter assay, demonstrated greater LIPTC GM volume increase after learning, which was also associated with greater verbal learning capacity change.

The hippocampal region was not identified to be associated with *AQP4* genetic variation in the voxel-wise analyses in either Sample 1 or Sample 2. The hippocampus not only shows high plasticity but also has great vulnerability to environmental stress and other factors.^{63,64} Particularly in Sample 2, with the intensive learning protocol, stress-induced atrophy from overuse may have occurred, which could well overcome the plastic changes induced by learning.⁶⁵ There was a discrepancy between the findings from a previous study by Martensson *et al.*,⁴¹ in which participants were military trainees exposed to a similar amount of foreign language learning as in our study. In their study, the inclusion of regular exercise in the protocol, which is one of the protective factors against stress-induced hippocampal atrophy,^{66,67} may have contributed to hippocampal volume increase.⁴¹

In the current study, the exact molecular mechanisms underlying the effects of allelic variation at SNP rs162008 on the gene-expression-level regulation have not been investigated. The 5'UTR, on which rs162008 is located, resides directly upstream from the initiation codon and is widely known for its critical role of regulating gene expression levels through various mechanisms, including the microRNA (miRNA)-mediated pathway.⁶⁸ For genes of which prompt changes in the expression level are required, translational regulation is particularly important to respond to milieu changes or external stimuli.⁶⁸ *AQP4*, considering its rapid downregulation or upregulation in response to internal and external stimuli,⁵⁸ could be one of the genes requiring these genetic switches.

Rs162008, the SNP tested in our investigation, is predicted to be bound by miRNAs according to the RegRNA software.⁶⁹ Intriguingly, binding potentials of miRNAs are modulated depending on the rs162008 SNP.⁶⁹ Although speculative, the binding of miRNAs to 5'UTR of *AQP4* when the T allele is present at rs162008, may inhibit gene expression. Further experiments are required to evaluate this hypothesis.

AQP4 being a novel candidate gene for brain plasticity and associated neuropsychiatric disorders, there is a paucity of existing literature, as anticipated, regarding the role of this gene in the pathogenesis of brain disorders with the exception of neurological conditions, such as neuromyelitis optica, epilepsy and brain edema related to stroke or traumatic brain injury.^{70,71} A line of indirect evidence supporting the role of *AQP4* genetic variation in the development of neuropsychiatric disorders may be found from genetic linkage analysis studies. The short arm of the chromosome 18, where *AQP4* resides, has repeatedly been implicated in the brain disorders of schizophrenia,¹⁷ attention-deficit hyperactivity disorder,²⁰ developmental delay, intellectual disability²¹ and autism spectrum disorders.²² *AQP4*, as one of the contributors among other multi-genetic factors, may be partly responsible for the reduced potential of brain plasticity and learning capacity, particularly with regard to the language-associated learning, in these disorders.

A pharmacological agent targeting the *AQP4* channel function may be developed as a novel therapeutic for enhancing astrocyte-modulated brain plasticity and learning in neuropsychiatric disorders. However, as *AQP4* may regulate multiple functions of astrocytes and is expressed in other organs such as the lung and thyroid gland, although at far lower concentrations than in the brain,⁷² potential side effects should be considered and prevented.

CONFLICT OF INTEREST

The authors declare no conflict of interest.

ACKNOWLEDGMENTS

This study was supported by grants from the Creative Research Initiative Program, National Research Foundation of Korea (2015R1A3A2066619), KIST Institutional Grant (2E26662), KU-KIST Graduate School of Science and Technology program (R1435281; to CJL), Fire Fighting Safety & 119 Rescue Technology Research and Development Program funded by the Ministry of Public Safety and Security (MPSS-Fire Fighting Safety-2016-86 (to JEK) and the Brain Research Program through the National Research Foundation of Korea, funded by the Ministry of Science, ICT and Future Planning (2015M3C7A1028373 and 2015M3C7A1028376; to IKL and JEK). We thank Siyoung Yu, MS, Sungeun Kim, MS, Heejung Hyun, MS, Yera Choi, MS, Eunji Ha, BS, Haejin Hong, BS, Suji L Lee, PharmD and Shinwon Park, MA for their technical assistance.

AUTHOR CONTRIBUTIONS

JW, JEK, IKL and CJL designed and supervised the study. JW, JEK, IKL and CJL wrote the manuscript with input from all authors. JW and JL performed electrophysiological experiments in mice. JEK, JJI, JM, IK and IKL coordinated the conduct of human studies. JEK, HSJ, SML, SL, JM and EYS analyzed the brain image data. JEK, HSJ, JM and IKL conducted and confirmed statistical analyses in human experiments. SP, HA, HC and BEY performed the immunohistochemistry. SYJ carried out luciferase assay. As an experienced neuroradiologist, SML screened all T1-weighted, T2-weighted and fluid-attenuated inversion recovery (FLAIR) images for any gross brain abnormalities. Non-brain tissues remaining after GM segmentation were removed by EYS. YEH developed the *AQP4* shRNA. BK, JM and EHL contributed to the genotyping data analyses and interpretation. LF analyzed the single astrocyte volume imaging data. JEK, JJI, HSJ, SY, SML, JM, EYS, IK, SRD and IKL participated in the interpretation of results from human data analyses. All authors provided critical intellectual contribution to the writing and revision of the manuscript.

REFERENCES

- 1 Szu JI, Binder DK. The role of astrocytic aquaporin-4 in synaptic plasticity and learning and Memory. *Front Integr Neurosci* 2016; **10**: 8.
- 2 Simard M, Nedergaard M. The neurobiology of glia in the context of water and ion homeostasis. *Neuroscience* 2004; **129**: 877–896.
- 3 Draganski B, Gaser C, Busch V, Schuierer G, Bogdahn U, May A. Neuroplasticity: changes in grey matter induced by training. *Nature* 2004; **427**: 311–312.
- 4 Kuhn S, Gleich T, Lorenz RC, Lindenberger U, Gallinat J. Playing Super Mario induces structural brain plasticity: gray matter changes resulting from training with a commercial video game. *Mol Psychiatry* 2014; **19**: 265–271.
- 5 Maguire EA, Gadian DG, Johnsrude IS, Good CD, Ashburner J, Frackowiak RS *et al*. Navigation-related structural change in the hippocampi of taxi drivers. *Proc Natl Acad Sci USA* 2000; **97**: 4398–4403.
- 6 Maguire EA, Woollett K, Spiers HJ. London taxi drivers and bus drivers: a structural MRI and neuropsychological analysis. *Hippocampus* 2006; **16**: 1091–1101.
- 7 Kempermann G, Kuhn HG, Gage FH. More hippocampal neurons in adult mice living in an enriched environment. *Nature* 1997; **386**: 493–495.
- 8 Susser ER, Wallace RB. The effects of environmental complexity on the hippocampal formation of the adult rat. *Acta Neurobiol Exp (Wars)* 1982; **42**: 203–207.
- 9 Lee DW, Miyasato LE, Clayton NS. Neurobiological bases of spatial learning in the natural environment: neurogenesis and growth in the avian and mammalian hippocampus. *Neuroreport* 1998; **9**: R15–R27.
- 10 Smulders TV, Sasson AD, DeVoogd TJ. Seasonal variation in hippocampal volume in a food-storing bird, the black-capped chickadee. *J Neurobiol* 1995; **27**: 15–25.
- 11 Fields RD. A new mechanism of nervous system plasticity: activity-dependent myelination. *Nat Rev Neurosci* 2015; **16**: 756–767.
- 12 Diamond MC, Scheibel AB, Murphy GM Jr, Harvey T. On the brain of a scientist: Albert Einstein. *Exp Neurol* 1985; **88**: 198–204.
- 13 Falk D, Lepore FE, Noe A. The cerebral cortex of Albert Einstein: a description and preliminary analysis of unpublished photographs. *Brain* 2013; **136**: 1304–1327.
- 14 Tait MJ, Saadoun S, Bell BA, Papadopoulos MC. Water movements in the brain: role of aquaporins. *Trends Neurosci* 2008; **31**: 37–43.
- 15 Wang YF, Parpura V. Central role of maladapted astrocytic plasticity in ischemic brain edema formation. *Front Cell Neurosci* 2016; **10**: 129.

- 16 Nielsen S, Nagelhus EA, Amiry-Moghaddam M, Bourque C, Agre P, Ottersen OP. Specialized membrane domains for water transport in glial cells: high-resolution immunogold cytochemistry of aquaporin-4 in rat brain. *J Neurosci* 1997; **17**: 171–180.
- 17 Williams NM, Rees MI, Holmans P, Norton N, Cardno AG, Jones LA et al. A two-stage genome scan for schizophrenia susceptibility genes in 196 affected sibling pairs. *Hum Mol Genet* 1999; **8**: 1729–1739.
- 18 Mathews CA, Reus VI. Genetic linkage in bipolar disorder. *CNS Spectr* 2003; **8**: 891–904.
- 19 Merette C, Bissonnette L, Rouillard E, Roy M, Maziade M. Positive linkage results for bipolar disorder on 18q in large kindreds from eastern Quebec (Abstract). *Am J Med Genet* 1997; **74**: 674.
- 20 Romanos M, Freitag C, Jacob C, Craig DW, Dempfle A, Nguyen TT et al. Genome-wide linkage analysis of ADHD using high-density SNP arrays: novel loci at 5q13.1 and 14q12. *Mol Psychiatry* 2008; **13**: 522–530.
- 21 Kaminsky EB, Kaul V, Paschall J, Church DM, Bunke B, Kunig D et al. An evidence-based approach to establish the functional and clinical significance of copy number variants in intellectual and developmental disabilities. *Genet Med* 2011; **13**: 777–784.
- 22 Isaksen J, Bryn V, Diseth TH, Heiberg A, Schjølberg S, Skjeldal OH. Children with autism spectrum disorders - the importance of medical investigations. *Eur J Paediatr Neurol* 2013; **17**: 68–76.
- 23 Arguello PA, Gogos JA. Genetic and cognitive windows into circuit mechanisms of psychiatric disease. *Trends Neurosci* 2012; **35**: 3–13.
- 24 Hackam DG, Redelmeier DA. Translation of research evidence from animals to humans. *JAMA* 2006; **296**: 1731–1732.
- 25 Lek M, Karczewski KJ, Minikel EV, Samocha KE, Banks E, Fennell T et al. Analysis of protein-coding genetic variation in 60,706 humans. *Nature* 2016; **536**: 285–291.
- 26 Ventura A, Meissner A, Dillon CP, McManus M, Sharp PA, Van Parijs L et al. Cre-lox-regulated conditional RNA interference from transgenes. *Proc Natl Acad Sci USA* 2004; **101**: 10380–10385.
- 27 Rosenzweig MR, Krech D, Bennett EL, Diamond MC. Effects of environmental complexity and training on brain chemistry and anatomy: a replication and extension. *J Comp Physiol Psychol* 1962; **55**: 429–437.
- 28 Cavalieri B. *Geometria Degli Indivisibili*. Unione Tipografica: Torino, Italy, 1966.
- 29 MacVicar BA, Hochman D. Imaging of synaptically evoked intrinsic optical signals in hippocampal slices. *J Neurosci* 1991; **11**: 1458–1469.
- 30 Woo DH, Han KS, Shim JW, Yoon BE, Kim E, Bae JY et al. TREK-1 and Best1 channels mediate fast and slow glutamate release in astrocytes upon GPCR activation. *Cell* 2012; **151**: 25–40.
- 31 Choe AY, Hwang ST, Kim JH, Park KB, Chey J, Hong SH. Validity of the K-WAIS-IV Short Forms. *Kor J Clin Psychol* 2014; **33**: 413–428.
- 32 Huang CC, Liu M-E, Kao H-W, Chou K-H, Yang AC, Wang Y-H et al. Effect of Alzheimer's disease risk variant rs3824968 at SORL1 on regional gray matter volume and age-related interaction in adult lifespan. *Sci Rep* 2016; **6**: 23362.
- 33 Smith SM, Jenkinson M, Woolrich MW, Beckmann CF, Behrens TE, Johansen-Berg H et al. Advances in functional and structural MR image analysis and implementation as FSL. *Neuroimage* 2004; **23**(Suppl 1): S208–S219.
- 34 FMRIB Software Library v5 0. Available at <https://fsl.fmrib.ox.ac.uk/fsl/fslwiki/> (Accessed 4 January 2017).
- 35 Smith SM. Fast robust automated brain extraction. *Hum Brain Mapp* 2002; **17**: 143–155.
- 36 West BT, Welch KB, Galecki AT. *Linear Mixed Models: A Practical Guide Using Statistical Software*. Chapman & Hall/CRC: Boca Raton, FL, USA, 2007.
- 37 AFNI program. 3dClustSim. Available at https://afni.nimh.nih.gov/pub/dist/doc/program_help/3dClustSim.html. Accessed 4 January 2017.
- 38 Bennett CM, Wolford GL, Miller MB. The principled control of false positives in neuroimaging. *Soc Cogn Affect Neurosci* 2009; **4**: 417–422.
- 39 Nichols TE. Multiple testing corrections, nonparametric methods, and random field theory. *Neuroimage* 2012; **62**: 811–815.
- 40 Benton AL, Hamsler KD, Sivan AB. Multilingual Aphasia Examination: Manual of Instructions 3rd (edn). AJA Associates: Iowa City, IA, USA, 1994.
- 41 Martensson J, Eriksson J, Bodammer NC, Lindgren M, Johansson M, Nyberg L et al. Growth of language-related brain areas after foreign language learning. *Neuroimage* 2012; **63**: 240–244.
- 42 Kim JK, Kang Y. Brief report normative study of the Korean-California Verbal Learning Test (K-CVLT). *Clin Neuropsychol* 1999; **13**: 365–369.
- 43 Delis DC, Kramer JH, Kaplan E, Ober BA. *CVLT, California Verbal Learning Test: Adult Version: Manual*. Psychological Corporation: San Antonio, TX, 1987.
- 44 Delis DC, Freeland J, Kramer JH, Kaplan E. Integrating clinical assessment with cognitive neuroscience: construct validation of the California Verbal Learning Test. *J Consult Clin Psychol* 1988; **56**: 123–130.
- 45 Skucas VA, Mathews IB, Yang J, Cheng Q, Treister A, Duffy AM et al. Impairment of select forms of spatial memory and neurotrophin-dependent synaptic plasticity by deletion of glial aquaporin-4. *J Neurosci* 2011; **31**: 6392–6397.
- 46 Penfield W, Roberts L. *Speech and Brain-Mechanisms*. Princeton University Press: NJ, USA, 1959.
- 47 Posner MI, Raichle ME. *Images of Mind*. Scientific American Library: NY, USA, 1994.
- 48 Benjamini Y, Hochberg Y. Controlling the false discovery rate: a practical and powerful approach to multiple testing. *J R Stat Soc* 1995; **57**: 289–300.
- 49 Cohen LB, Keynes RD. Changes in light scattering associated with the action potential in crab nerves. *J Physiol* 1971; **212**: 259–275.
- 50 Nedergaard M, Ransom B, Goldman SA. New roles for astrocytes: redefining the functional architecture of the brain. *Trends Neurosci* 2003; **26**: 523–530.
- 51 Li YK, Wang F, Wang W, Luo Y, Wu PF, Xiao JL et al. Aquaporin-4 deficiency impairs synaptic plasticity and associative fear memory in the lateral amygdala: involvement of downregulation of glutamate transporter-1 expression. *Neuropsychopharmacology* 2012; **37**: 1867–1878.
- 52 Fan Y, Liu M, Wu X, Wang F, Ding J, Chen J et al. Aquaporin-4 promotes memory consolidation in Morris water maze. *Brain Struct Funct* 2013; **218**: 39–50.
- 53 Yang J, Li MX, Luo Y, Chen T, Liu J, Fang P et al. Chronic ceftriaxone treatment rescues hippocampal memory deficit in AQP4 knockout mice via activation of GLT-1. *Neuropharmacology* 2013; **75**: 213–222.
- 54 Papadopoulos MC, Verkman AS. Aquaporin water channels in the nervous system. *Nat Rev Neurosci* 2013; **14**: 265–277.
- 55 Gorelick DA, Praetorius J, Tsunenari T, Nielsen S, Agre P. Aquaporin-11: a channel protein lacking apparent transport function expressed in brain. *BMC Biochem* 2006; **7**: 14.
- 56 Nagelhus EA, Ottersen OP. Physiological roles of aquaporin-4 in brain. *Physiol Rev* 2013; **93**: 1543–1562.
- 57 Allen Brain Atlas. Available at <http://www.brain-map.org/>. Accessed 8 February 2017.
- 58 Friedman B, Schachtrup C, Tsai PS, Shih AY, Akassoglou K, Kleinfeld D et al. Acute vascular disruption and aquaporin 4 loss after stroke. *Stroke* 2009; **40**: 2182–2190.
- 59 Li P, Legault J, Litcofsky KA. Neuroplasticity as a function of second language learning: anatomical changes in the human brain. *Cortex* 2014; **58**: 301–324.
- 60 Mamiya PC, Richards TL, Coe BP, Eichler EE, Kuhl PK. Brain white matter structure and *COMT* gene are linked to second-language learning in adults. *Proc Natl Acad Sci USA* 2016; **113**: 7249–7254.
- 61 Rapcsak SZ, Beeson PM. The role of left posterior inferior temporal cortex in spelling. *Neurology* 2004; **62**: 2221–2229.
- 62 Nakamura K, Honda M, Okada T, Hanakawa T, Toma K, Fukuyama H et al. Participation of the left posterior inferior temporal cortex in writing and mental recall of kanji orthography: a functional MRI study. *Brain* 2000; **123**(Pt 5): 954–967.
- 63 Kim JJ, Diamond DM. The stressed hippocampus, synaptic plasticity and lost memories. *Nat Rev Neurosci* 2002; **3**: 453–462.
- 64 McEwen BS. Stress and hippocampal plasticity. *Annu Rev Neurosci* 1999; **22**: 105–122.
- 65 Draganski B, Gaser C, Kempermann G, Kuhn HG, Winkler J, Buchel C et al. Temporal and spatial dynamics of brain structure changes during extensive learning. *J Neurosci* 2006; **26**: 6314–6317.
- 66 Adlars PA, Cotman CW. Voluntary exercise protects against stress-induced decreases in brain-derived neurotrophic factor protein expression. *Neuroscience* 2004; **124**: 985–992.
- 67 Erickson KI, Voss MW, Prakash RS, Basak C, Szabo A, Chaddock L et al. Exercise training increases size of hippocampus and improves memory. *Proc Natl Acad Sci USA* 2011; **108**: 3017–3022.
- 68 Araujo PR, Yoon K, Ko D, Smith AD, Qiao M, Suresh U et al. Before it gets started: regulating translation at the 5' UTR. *Comp Funct Genomics* 2012; **2012**: 475731.
- 69 Huang HD. *A Regulatory RNA Motifs and Elements Finder*. Available at <http://regna.mbc.nctu.edu.tw/index1.php>. Accessed 18 February 2017.
- 70 Lan YL, Fang DY, Zhao J, Ma TH, Li S. A research update on the potential roles of aquaporin 4 in neuroinflammation. *Acta Neurol Belg* 2016; **116**: 127–134.
- 71 Xiao M, Hu G. Involvement of aquaporin 4 in astrocyte function and neuropsychiatric disorders. *CNS Neurosci Ther* 2014; **20**: 385–390.
- 72 The Broad Institute of MIT and Harvard. GTEx Portal. Available at <http://www.gtexportal.org/home/gene/AQP4>. Accessed 14 February 2017.

Supplementary Information accompanies the paper on the Molecular Psychiatry website (<http://www.nature.com/mp>)